

Entanglement and quantum discord in the cavity QED models

Miao Hui-hui* and Li Wan-shun

*Faculty of Computational Mathematics and Cybernetics,
Lomonosov Moscow State University, Vorobyovy Gory 1, Moscow, 119991, Russia*

(Dated: March 12, 2024)

Based on the two-qubit Jaynes–Cummings model — a common cavity quantum electrodynamics model, and extending to modification of the three-qubit Tavis–Cummings model, we investigate the quantum correlation between light and matter in bipartite quantum systems. By resolving the quantum master equation, we are able to derive the dissipative dynamics in open systems. To gauge the degree of quantum entanglement, some entanglement measurements are introduced: von Neumann entropy, concurrence and quantum discord. In addition, consideration is given to the impacts of initial entanglement and dissipation strength on quantum discord. Finally we discussed two different cases of nuclei motion: quantum and classical.

Keywords: finite-dimensional QED, entanglement, quantum discord, entropy, concurrence.

I. INTRODUCTION

The Einstein–Podolsky–Rosen (EPR) paradox put out by Einstein et al. [1] served as the inspiration for the idea of quantum entanglement [2]. The study of fundamental problems in quantum information theory has always focused heavily on quantum entanglement. Quantum information processing (QIP), which is related to entanglement, provides a larger variety of information manipulation techniques than the conventional approach. Lacking a classical counterpart, the quantum entanglement is unique and has been seen as a key resource for QIP, including quantum computation [3], quantum cryptography [4], and other works [5, 6]. However, according to the current theory, quantum entanglement is merely a particular type of quantum correlation, which is a more fundamental idea than quantum entanglement [7, 8]. The correlation that contains both classical and quantum components may be more extensive and basic than entanglement. The quantum discord is a novel but interesting candidate of quantum correlation, which was first proposed by Ollivier and Zurek [8, 9], explained in detail by Vedral et al. [7, 10, 11], and introduced into many fields for research recently [12–21]. Similar to quantum entanglement, the quantum correlation will continue to attenuate under the effect of external environmental noise, which is the process of quantum decoherence. The decoherence process is unavoidable since the actual quantum system is not an entirely closed ideal system. How to deal with decoherence, which is the major obstacle to the superiority of QIP, is the main issue.

The quantum electrodynamics (QED) model, which presents a distinct physical paradigm for examining interaction between light and matter, is a fundamental contribution to this paper. In this paradigm, fields of cavities are coupled to impurity two- or multi-level systems, which are typically referred to as atoms. The most studied cavity QED model is the Jaynes–Cummings

model (JCM) [22] and its generalizations and modifications [23, 24], which are typically easier to realize in experiment. In the last time a lot of research has been carried out in the area of cavity QED models [25–33]. Previous studies have rarely involved quantum correlation in cavity QED systems. Sometimes quantum correlation can be used for certain quantum calculations. Thus, the study of quantum correlation dynamics in the cavity QED systems is very necessary.

We investigate the quantum entanglement via von Neumann entropy and concurrence in bipartite systems, based on the two- and three-qubit cavity QED models (JCM and Tavis–Cummings model (TCM), respectively). Consideration is also given to the quantum discord. We can obtain the dissipative dynamics in open systems by solving the quantum master equation (QME). We study the quantum entanglement and compare it with quantum discord. We also investigate the impact of initial entanglement and dissipation strength on quantum discord. Finally we discussed the quantum and classical motion of nuclei.

This paper is organized as follows. After introducing the basic principles of the quantum theory of information, and the definitions of von Neumann entropy, concurrence and quantum discord in Sec. II, we introduce in succession two-qubit JCM and three-qubit TCM in Sec. III and Sec. IV, respectively. We do the numerical simulations and get some results in Sec. V. Some brief comments on our results and extension to future work in Sec. VI close out the paper. List of abbreviations and notations used in this paper is put in Appendix A.

II. CORRELATION IN QUANTUM SYSTEM

A. Quantum entanglement

When a group of particles are created, interact, or share spatial proximity in a way that prevents each particle's quantum state from being independently described from the states of the others, this phenomenon known

* Email address: hhmiao@cs.msu.ru

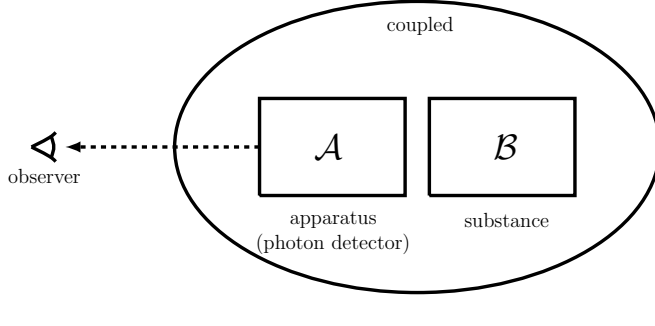


FIG. 1. (online color) *Coupling system of apparatus and substance*. We separate the quantum system into two subsystems: the observation system \mathcal{A} and the substance system \mathcal{B} . In this paper, the substance system corresponds to electrons and atomic nuclei, and the part observed by the apparatus is photons (here observer uses a photon detector to capture photons). Subsystems \mathcal{A} and \mathcal{B} are coupled together into a whole by the field in the optical cavity.

as quantum entanglement takes place. Quantum entanglement occurs even when the particles are separated by a great distance. The fundamental difference between classical and quantum physics is the issue of quantum entanglement, which is a key aspect of quantum mechanics that is absent from classical mechanics. The following singlet state of two-spin system is the most prevalent type of quantum entanglement

$$|\Psi\rangle = \frac{1}{\sqrt{2}}(|\uparrow\downarrow\rangle - |\downarrow\uparrow\rangle) \quad (1)$$

where \uparrow — spin up and \downarrow — spin down.

For a bipartite system, we set the observed subsystem as \mathcal{A} and the unobserved subsystem as \mathcal{B} . As shown in Fig. 1, it is more convenient to detect photons in the cavity QED model than to detect other particles.

In simulations, we divide the measurement of quantum entanglement into two cases for discussion: closed and open quantum system. We introduce von Neumann entropy and concurrence to measure the degree of entanglement.

1. von Neumann entropy

When the quantum system is closed, the whole system is in pure state $|pure\rangle$, then we can directly use the von Neumann entropy of reduced density matrix, which is used to measure quantum correlation, but it can be regarded as entropy of entanglement when system is closed. In this case, due to the Schmidt decomposition, the von Neumann entropy of each of two subsystems \mathcal{A} and \mathcal{B} can be used as a gauge of the system's entanglement [34]

$$E = S(\mathcal{A}) = S(\mathcal{B}) \quad (2)$$

where $S(\mathcal{A})$, $S(\mathcal{B})$ are corresponding to $\rho_{\mathcal{A}}$, $\rho_{\mathcal{B}}$, respectively. And $\rho_{\mathcal{A}(\mathcal{B})}$ — reduction of density matrix $\rho_{\mathcal{A}\mathcal{B}}$, which is the density matrix of whole system, has the following form

$$\begin{aligned} \rho_{\mathcal{A}} &= Tr_{\mathcal{B}}(\rho_{\mathcal{A}\mathcal{B}}) \\ &= \sum_b (I_{\mathcal{A}} \otimes \langle b|_{\mathcal{B}}) \rho_{\mathcal{A}\mathcal{B}} (I_{\mathcal{A}} \otimes |b\rangle_{\mathcal{B}}) \end{aligned} \quad (3a)$$

$$\begin{aligned} \rho_{\mathcal{B}} &= Tr_{\mathcal{A}}(\rho_{\mathcal{A}\mathcal{B}}) \\ &= \sum_a (\langle a|_{\mathcal{A}} \otimes I_{\mathcal{B}}) \rho_{\mathcal{A}\mathcal{B}} (|a\rangle_{\mathcal{A}} \otimes I_{\mathcal{B}}) \end{aligned} \quad (3b)$$

and

$$\rho_{\mathcal{A}\mathcal{B}} = |pure\rangle\langle pure| \quad (4)$$

In quantum theory, the definition of von Neumann entropy of reduced density matrix $\rho_{\mathcal{A}(\mathcal{B})}$ is as follows

$$S(\mathcal{A}(\mathcal{B})) = -Tr(\rho_{\mathcal{A}(\mathcal{B})} \log_2 \rho_{\mathcal{A}(\mathcal{B})}) \quad (5)$$

In terms of eigenvalues, we have

$$S(\mathcal{A}(\mathcal{B})) = - \sum_i \lambda_i^{\mathcal{A}(\mathcal{B})} \log_2 \lambda_i^{\mathcal{A}(\mathcal{B})} \quad (6)$$

where $\lambda_i^{\mathcal{A}(\mathcal{B})}$ — eigenvalues of density matrix $\rho_{\mathcal{A}(\mathcal{B})}$. $0 \leq S(\mathcal{A}(\mathcal{B})) \leq \log_2 N$, $N = 2^n$, N — Hilbert space dimension, n — number of qubits. $S(\mathcal{A}(\mathcal{B})) = 0$ — separable state, $S(\mathcal{A}(\mathcal{B})) > 0$ — entangled state, $S(\mathcal{A}(\mathcal{B})) = \log_2 N$ — maximum entangled state.

2. Concurrence

Now we review concurrence for the two-qubit system, especially when the system is dissipative (at this point, the whole system is in a mixed state), to measure the entanglement. Concurrence describes the two-qubit entanglement as

$$C = \max\{\sqrt{\lambda_3} - \sqrt{\lambda_2} - \sqrt{\lambda_1} - \sqrt{\lambda_0}, 0\} \quad (7)$$

This equation is also called Hill–Wootters equation [35–37]. Here λ_1 , λ_2 , λ_3 and λ_4 are matrix eigenvalues of $\tilde{\rho}_{\mathcal{A}\mathcal{B}}$, and $\lambda_3 > \lambda_2 > \lambda_1 > \lambda_0 \geq 0$. Density matrix $\tilde{\rho}_{\mathcal{A}\mathcal{B}}$ has the following form

$$\tilde{\rho}_{\mathcal{A}\mathcal{B}} = \rho_{\mathcal{A}\mathcal{B}} (\sigma_y \otimes \sigma_y) \rho_{\mathcal{A}\mathcal{B}}^* (\sigma_y \otimes \sigma_y)^\dagger \quad (8)$$

where $\rho_{\mathcal{A}\mathcal{B}}^*$ — complex conjugation of a matrix $\rho_{\mathcal{A}\mathcal{B}}$. $\sigma_y = -i|0\rangle\langle 1| + i|1\rangle\langle 0|$. $C = 0$ — separable state, $C > 0$ — entangled state, $C = 1$ — maximum entangled state.

B. Quantum discord

Quantum discord is a measure of nonclassical correlations between two subsystems of a quantum system used in quantum information theory. It also contains correlations resulting from quantum physical phenomena but not necessarily from quantum entanglement. Moreover, it serves as a gauge for the quantumness of correlations.

1. Overall correlation

Firstly, we introduce the concepts of Shannon's theory into the field of quantum informatics. In classical information theory, the information can be quantified by Shannon entropy

$$H(X) = \sum_x P_{|X=x} \ln P_{|X=x} \quad (9)$$

where $P_{|X=x}$ is the probability with X being x . For two random variables X and Y , the total correlation between them can be measured by the mutual information which is defined as

$$I(X : Y) = H(X) + H(Y) - H(X, Y) \quad (10)$$

We extend the above equation to the field of quantum information, and obtain the equation of quantum mutual information

$$\begin{aligned} \mathcal{I}(\mathcal{B} : \mathcal{A}) &= S(\mathcal{A}) + S(\mathcal{B}) - S(\mathcal{A}\mathcal{B}) \\ &= \mathcal{I}(\mathcal{A} : \mathcal{B}) \end{aligned} \quad (11)$$

where $S(\mathcal{A}\mathcal{B})$ — von Neumann entropy for the system $\rho_{\mathcal{A}\mathcal{B}}$, $S(\mathcal{A})$ — entropy for the subsystem $\rho_{\mathcal{A}}$, $S(\mathcal{B})$ — entropy for the subsystem $\rho_{\mathcal{B}}$. $\mathcal{I}(\mathcal{B} : \mathcal{A})$ describes the overall correlation of the system.

2. Classical correlation

Then $\mathcal{J}(\mathcal{B} : \mathcal{A})$, which describes the maximum classical correlation, is introduced. It has the following form

$$\begin{aligned} \mathcal{J}(\mathcal{B} : \mathcal{A}) &= \max_{\{\Pi_k^{\mathcal{A}}\}} [S(\mathcal{B}) - S(\mathcal{B}|\mathcal{A})] \\ &= \max_{\{\Pi_k^{\mathcal{A}}\}} [S(\mathcal{B}) - \sum_k p_k S(\rho_k)] \\ &= S(\mathcal{B}) - \min_{\{\Pi_k^{\mathcal{A}}\}} \sum_k p_k S(\rho_k) \end{aligned} \quad (12)$$

where $\{\Pi_k^{\mathcal{A}}\}$ is a complete set of projectors for the von Neumann projective measurement (orthogonal projection basis) of subsystem \mathcal{A} . The von Neumann projective measurement basis for a Hilbert space with dimension 2 (one qubit) is as follows

$$\{|b_k\rangle\} = \{|\cos\theta|0\rangle + |\sin\theta|1\rangle, |\sin\theta|0\rangle - |\cos\theta|1\rangle\} \quad (13)$$

where $\theta \in [0, \frac{\pi}{2}]$ and projection operators

$$\begin{aligned} \Pi_0^{\mathcal{A}} &= \cos^2\theta|0\rangle\langle 0| + \cos\theta\sin\theta|0\rangle\langle 1| \\ &\quad + \cos\theta\sin\theta|1\rangle\langle 0| + \sin^2\theta|1\rangle\langle 1| \end{aligned} \quad (14a)$$

$$\begin{aligned} \Pi_1^{\mathcal{A}} &= \sin^2\theta|0\rangle\langle 0| - \cos\theta\sin\theta|0\rangle\langle 1| \\ &\quad - \cos\theta\sin\theta|1\rangle\langle 0| + \cos^2\theta|1\rangle\langle 1| \end{aligned} \quad (14b)$$

The von Neumann projective measurement basis in Eq. (13) can be extended to

$$\{|b_k\rangle\} = \{|\cos\theta|0\rangle + |\sin\theta e^{i\varphi}|1\rangle, |\sin\theta e^{-i\varphi}|0\rangle - |\cos\theta|1\rangle\} \quad (15)$$

where $\varphi \in [0, 2\pi]$.

After constructing the projection operators of subsystem \mathcal{A} , we can measure it and get ρ_k , which is defined as follows

$$\rho_k = \text{Tr}_{\mathcal{A}}[(\Pi_k^{\mathcal{A}} \otimes I_{\mathcal{B}})\rho_{\mathcal{A}\mathcal{B}}(\Pi_k^{\mathcal{A}} \otimes I_{\mathcal{B}})^\dagger]/p_k \quad (16)$$

where

$$p_k = \text{Tr}[(\Pi_k^{\mathcal{A}} \otimes I_{\mathcal{B}})\rho_{\mathcal{A}\mathcal{B}}(\Pi_k^{\mathcal{A}} \otimes I_{\mathcal{B}})^\dagger] \quad (17)$$

ρ_k is the state of the subsystem \mathcal{B} after a measurement of subsystem \mathcal{A} leading to an outcome k with a probability p_k .

It should be noted that in most cases $\mathcal{J}(\mathcal{B} : \mathcal{A})$ is not equal to $\mathcal{J}(\mathcal{A} : \mathcal{B})$, described as follows

$$\begin{aligned} \mathcal{J}(\mathcal{A} : \mathcal{B}) &= \max_{\{\Pi_{k'}^{\mathcal{B}}\}} [S(\mathcal{A}) - S(\mathcal{A}|\mathcal{B})] \\ &= \max_{\{\Pi_{k'}^{\mathcal{B}}\}} [S(\mathcal{A}) - \sum_{k'} p_{k'} S(\rho_{k'})] \\ &= S(\mathcal{A}) - \min_{\{\Pi_{k'}^{\mathcal{B}}\}} \sum_{k'} p_{k'} S(\rho_{k'}) \end{aligned} \quad (18)$$

where

$$\rho_{k'} = \text{Tr}_{\mathcal{B}}[(I_{\mathcal{A}} \otimes \Pi_{k'}^{\mathcal{B}})\rho_{\mathcal{A}\mathcal{B}}(I_{\mathcal{A}} \otimes \Pi_{k'}^{\mathcal{B}})^\dagger]/p_{k'} \quad (19)$$

$$p_{k'} = \text{Tr}[(I_{\mathcal{A}} \otimes \Pi_{k'}^{\mathcal{B}})\rho_{\mathcal{A}\mathcal{B}}(I_{\mathcal{A}} \otimes \Pi_{k'}^{\mathcal{B}})^\dagger] \quad (20)$$

3. Quantum correlation

Now we define that the quantum discord is the difference between the total correlation and the maximum of classical correlation

$$\mathcal{D}(\mathcal{B} : \mathcal{A}) = \mathcal{I}(\mathcal{B} : \mathcal{A}) - \mathcal{J}(\mathcal{B} : \mathcal{A}) \quad (21)$$

where $0 \leq \mathcal{D}(\mathcal{B} : \mathcal{A}) < \mathcal{I}(\mathcal{B} : \mathcal{A})$, $\mathcal{D}(\mathcal{B} : \mathcal{A}) \leq S(\mathcal{A})$. As in the case of the maximum classical correlation, $\mathcal{D}(\mathcal{B} : \mathcal{A})$ is not equal to $\mathcal{D}(\mathcal{A} : \mathcal{B})$ in most cases. The physical meaning of discord is that the greater $\mathcal{D}(\mathcal{B} : \mathcal{A})$, the greater the minimum loss of information in the subsystem \mathcal{B} after measurement of subsystem \mathcal{A} . In other words, the greater the minimum disturbance caused to subsystem \mathcal{B} after measuring the subsystem \mathcal{A} , the stronger the correlation between \mathcal{B} and \mathcal{A} .

The maximization in $\mathcal{J}(\mathcal{B} : \mathcal{A})$ represents the most information obtained about the system \mathcal{B} as a result of perfect measurement $\{\Pi_k^{\mathcal{A}}\}$. It can be shown that the quantum discord is zero for states with only classical correlation and nonzero for states with quantum correlation.

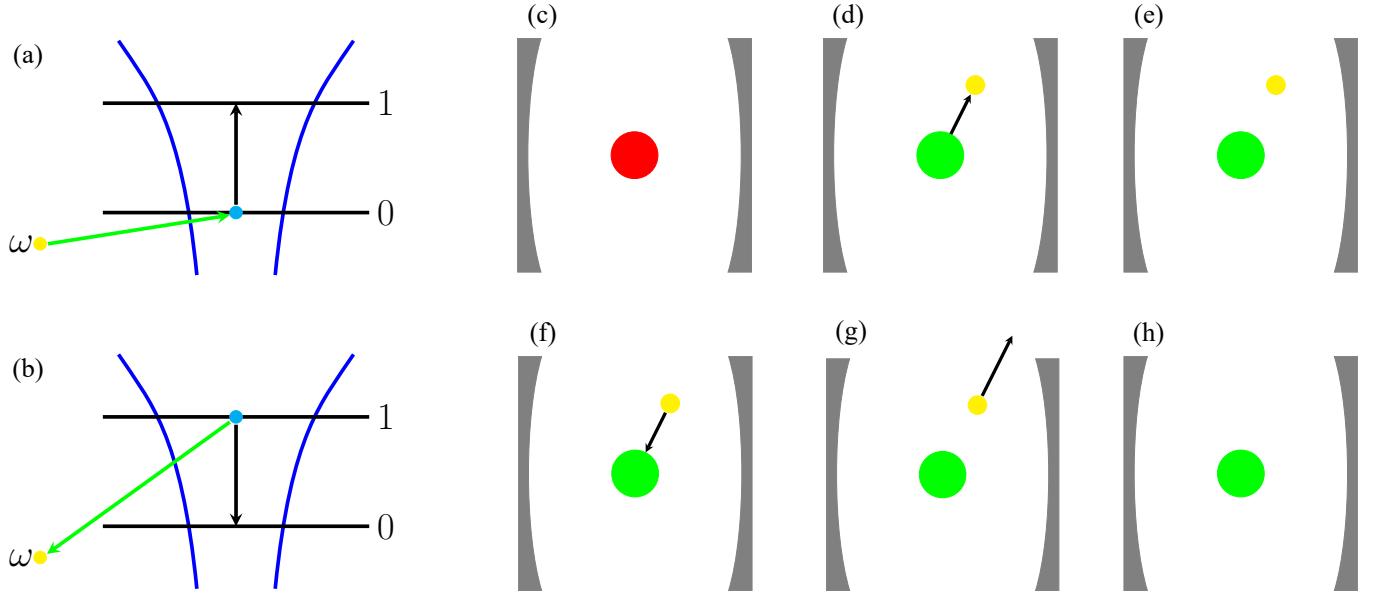


FIG. 2. (online color) *Schematic diagram of the Jaynes-Cummings model.* (a) and (b) represent in detail the excitation and de-excitation processes of a two-level atom, respectively. (c) ~ (h) represent the three states of the JCM, the interaction between the atom and the field, and the dissipation effect of the system. Among them, (c), (e), and (h) represent the three quantum states of the system: $|01\rangle$, $|10\rangle$, and $|00\rangle$, respectively. (d) represents the de-excitation, (f) represents the excitation, and (g) represents the photon escape. The yellow dot stands for photon. Electron is seen in (a) and (b) as blue dot. Excited atom and ground state atom are seen in (c) ~ (h) as red and green dot, respectively.

III. TWO-QUBIT JAYNES-CUMMINGS MODEL

In this paper, we investigate quantum entanglement and quantum discord dynamics on two cavity QED models. First, we introduce the two-qubit JCM.

The JCM is a theoretical quantum optics model. It explains the interaction between a two-level atom and a quantized mode of an optical cavity. In order to better understand the phenomena of spontaneous emission and photon absorption in a cavity, it was initially designed to examine how atoms interact with the quantized electromagnetic field. Atomic physics, quantum optics, solid-state physics, and QIP all have a lot of theoretical and experimental interest in the JCM.

The basic states of the JCM system is as follow

$$|\Psi\rangle = \underbrace{|p\rangle_{ph}}_{\mathcal{A}} \underbrace{|l\rangle_{at}}_{\mathcal{B}} \quad (22)$$

where $p = 0$ — no free photons, $p = 1$ — one free photon, $l = 0$ — electron in ground state, $l = 1$ — electron in excited state. The photon state is partly viewed as the observed by photon detector.

Interaction between atom and field is explained in detail in Fig. 2. In (a), an electron in the ground state absorbs a photon and transfer to the excited state, which is called excitation. In (b), an electron in the excited state transfer to the ground state after releasing a photon, this process is called de-excitation. (c), (e), (h) correspond re-

spectively to three states for JCM: $|01\rangle$, $|10\rangle$, $|00\rangle$. Excitation process is shown as

$$(e) \xrightarrow{(f)} (c)$$

De-excitation process is shown as

$$(c) \xrightarrow{(d)} (e)$$

If the optical cavity is ideal, then the entire system is closed, and the state of the system will oscillate between (c) and (e), since there is no photon leakage (dissipation). The quantum discord is currently greater than or equal to zero, and the system comprises of the entangled state of $|01\rangle$ and $|10\rangle$. The quantum discord is zero when one of the probabilities of $|01\rangle$ and $|10\rangle$ is zero. However, the optical cavity is not ideal in reality, known as open system, and photons will escape from the cavity to the external environment. Dissipation process is shown as

$$(e) \xrightarrow{(g)} (h)$$

The atoms in the cavity will ultimately stabilize in the ground state $|00\rangle$ due to photon leakage, which means that the system will no longer have quantum correlation and the quantum discord will be zero.

A. Hamiltonian of JCM

Before constructing the Hamiltonian, we first introduce rotating wave approximation (RWA) [38], which is

taken into account

$$\frac{g}{\hbar\omega_a} \approx \frac{g}{\hbar\omega_c} \ll 1 \quad (23)$$

Usually, for convenience, we assume that the electron transition frequency ω_a and field frequency ω_c are equal, and $\omega = \omega_a = \omega_c$. And Hamiltonian of JCM has following form

$$H_{JCM}^{RWA} = \hbar\omega a^\dagger a + \hbar\omega\sigma^\dagger\sigma + g(a^\dagger\sigma + a\sigma^\dagger) \quad (24)$$

where \hbar is the reduced Planck constant, g is the coupling intensity between the photonic mode ω and the electron in the molecule. Here a is photon annihilation operator, a^\dagger is photon creation operator, σ is electron excitation operator, and σ^\dagger is electron relaxation operator.

The coupling intensity of photon and the electron in the cavity takes the form:

$$g = \sqrt{\hbar\omega/V}dE(x) \quad (25)$$

where ω is transition frequency, V is the effective volume of the cavity, d is the dipole moment of the transition between the ground and the perturbed states and $E(x)$ describes the spatial arrangement of the atom in the cavity, which has the form $E(x) = \sin(\pi x/l)$, here l is the length of the cavity. To ensure the confinement of the photon in the cavity, l has to be chosen such that $l = m\lambda/2$ is a multiple of the photon wavelength λ . In experiments, $m = 1$ is often chosen to decrease the effective volume of the cavity, which makes it possible to obtain dozens of Rabi oscillations [39].

B. Quantum master equation

The QME in the Markovian approximation for the density operator ρ of the open system takes the following form

$$i\hbar\dot{\rho} = [H, \rho] + iL(\rho) \quad (26)$$

where $[H, \rho] = H\rho - \rho H$ is the commutator. $L(\rho)$ is as follows

$$L(\rho) = \sum_k \gamma_k \left(A_k \rho A_k^\dagger - \frac{1}{2} \left\{ \rho, A_k^\dagger A_k \right\} \right) \quad (27)$$

where $\left\{ \rho, A_k^\dagger A_k \right\} = \rho A_k^\dagger A_k + A_k^\dagger A_k \rho$ is the anticommutators, and A_k is jump operator. The term γ_k refers to the overall spontaneous emission rate for photons for k caused by photon leakage from the cavity to the external environment.

IV. THREE-QUBIT TAVIS–CUMMINGS MODEL

The OH^+ model within the framework of TCM is an extension of JCM. In the optical cavity exist two artificial

two-level atoms, one of them is hydrogen atom, another is oxygen atom. And there is only one valence electron between them. The hybridization and de-hybridization of orbitals is shown in Fig. 3 (a). Each atom has a structure similar to that in Sec. III. The excitation and de-excitation are shown in Fig. 3 (b) and (c). Electron in atomic ground orbital $|0\rangle_O$ (or $|0\rangle_H$) is bound to the nucleus and not participating in the formation of chemical bonds. Only when the electron is in atomic excited state $|1\rangle_O$ (or $|1\rangle_H$), atomic orbitals can be hybridized into molecular orbitals — the ground $|\Phi_0\rangle$ and excited $|\Phi_1\rangle$ ones

$$|\Phi_0\rangle = \alpha |1\rangle_O + \beta |1\rangle_H \quad (28a)$$

$$|\Phi_1\rangle = \beta |1\rangle_O - \alpha |1\rangle_H \quad (28b)$$

where α and β are positive coefficients depend on depth of potential wells in atoms, $\alpha \geq \beta$, $\alpha^2 + \beta^2 = 1$.

There is only one valence electron in the model, the basic state is denoted as follows:

$$|\psi\rangle = \underbrace{|p\rangle_{ph}}_{\mathcal{A}} \underbrace{|l\rangle_{mol}}_{\mathcal{B}} |k\rangle_n \quad (29)$$

where p — number of photons, $n = 0, 1$; $l = 0$ — $|\Phi_0\rangle$, $l = 1$ — $|\Phi_1\rangle$; $k = 0$ means the nuclei are close from each other (at this point covalent bond is strong), and $k = 1$ means far away (at this point covalent bond is weak).

Fig. 3 details the interactions and dissipations of the OH^+ model. (d) ~ (i) correspond to six states for OH^+ model: $|000\rangle$, $|001\rangle$, $|010\rangle$, $|011\rangle$, $|100\rangle$, $|101\rangle$. Excitation processes are shown as

$$(h) \xrightarrow{(k)} (f), (i) \xrightarrow{(m)} (g)$$

De-excitation processes are shown as

$$(f) \xrightarrow{(j)} (h), (g) \xrightarrow{(l)} (i)$$

And dissipation processes are shown as

$$(h) \xrightarrow{(n)} (d), (i) \xrightarrow{(o)} (e)$$

A. Hamiltonian of the OH^+ model

Hamiltonian of the OH^+ model has following form

$$H_{\text{OH}^+}^{RWA} = \hbar\omega_c a^\dagger a + \hbar\omega_b \sigma_b^\dagger \sigma_b + \hbar\omega_a \sigma_a^\dagger \sigma_a + g_b (\sigma_b + \sigma_b^\dagger) + g_a (a^\dagger \sigma_a + a \sigma_a^\dagger) \quad (30)$$

where a , a^\dagger — photon annihilation and creation operators; σ_b , σ_b^\dagger — covalent bond breaking and formation operator, σ_a , σ_a^\dagger — electron relaxation and excitation operator; ω_c — photon frequency in the cavity; ω_b — phonon frequency, corresponding to the energy of covalent bond; ω_a — atomic transition frequency, and $\omega_c = \omega_a = \omega$; g_b — intensity of formation of covalent bond; g_a — intensity of interaction of a molecule with the field.

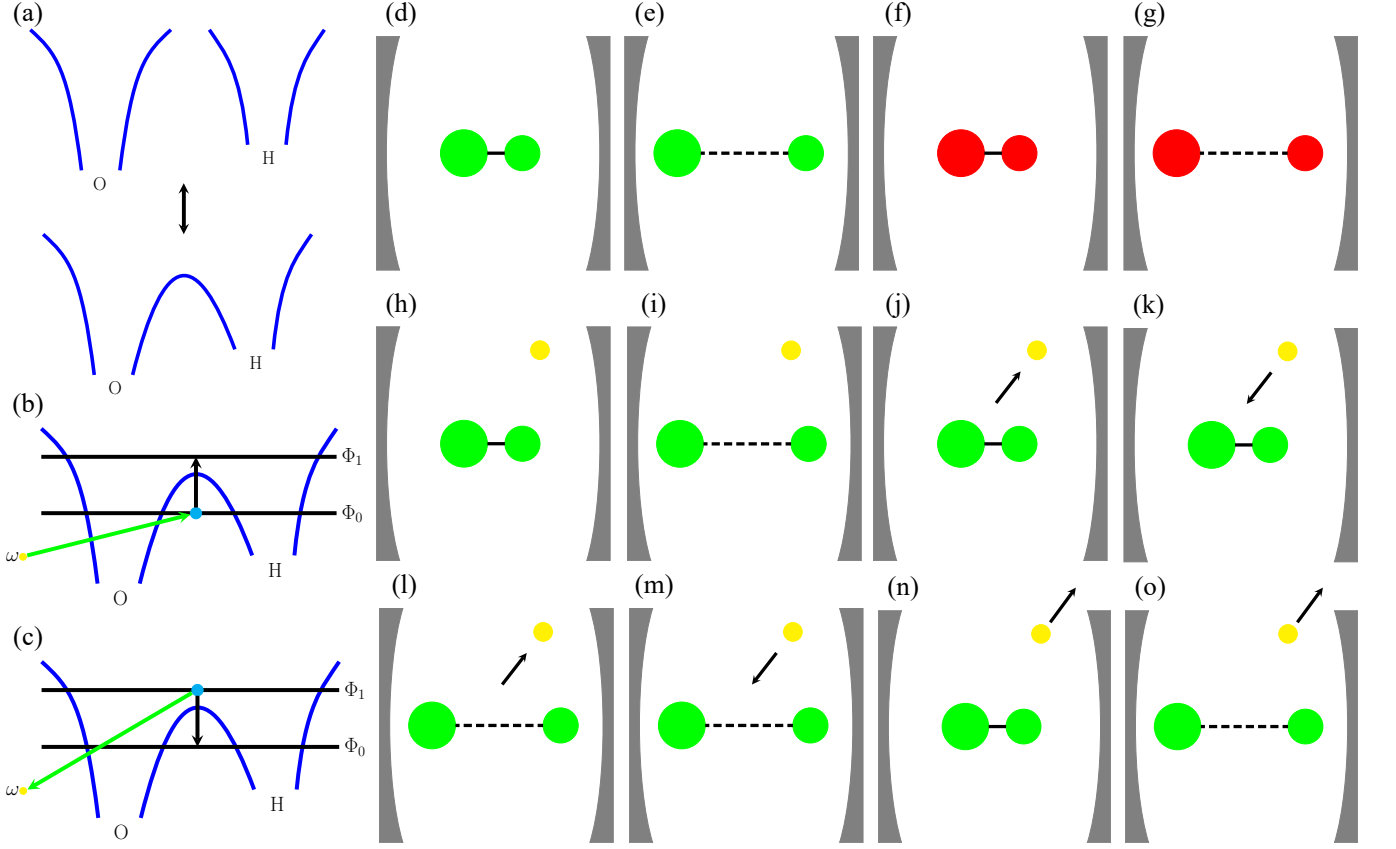


FIG. 3. (online color) *Schematic diagram of OH^+ model.* (a) represents the formation and breaking of covalent bond between atoms O and H. (b) and (c) represent in detail the excitation and de-excitation processes, respectively. (d) ~ (i) correspond to six states for OH^+ model: $|\text{000}\rangle$, $|\text{001}\rangle$, $|\text{010}\rangle$, $|\text{011}\rangle$, $|\text{100}\rangle$, $|\text{101}\rangle$; (j) ~ (m) represent interactions; (n), (o) represent dissipations. Two circles are connected by a solid or dashed line. The large circle represents oxygen atom and the small circle represents hydrogen atom. The solid line indicates a strong covalent bond (when the two atoms are close together), the dashed line indicates a weak covalent bond (when the two atoms are far apart). The other symbols are the same as those in Fig. 2.

When electron is in the excited state, the system will be more unstable than when in the ground state. This means that covalent bond is more easily broken or formed. At this time, $g_b = g_{b_1}$, which is large. When electron is in the ground state, the system will be more stable. It will be difficult to form or break covalent bonds. At this time, $g_b = g_{b_0}$, which is weak, and $g_{b_1} \gg g_{b_0}$.

In addition, we stipulate that when the distance between two atoms is close, the covalent bond is strong (this means that the diatomic system tends towards the molecular form), at this time, $g_a = g_{a_0}$, which is large; when the distance is far, the covalent bond is weak (this means that the diatomic system tends towards the independent atoms form), at this time, $g_a = g_{a_1}$, which is weak. We assume $g_{a_1} \ll g_{a_0}$.

The quantum master equation of the OH^+ model is similar to that in Subsec. III B.

V. SIMULATIONS AND RESULTS

In this paper, quantum evolutions are schematically modelled by solving the QME with the Lindblad operators. QME approach has been used to study the dynamics of quantum open system [40], and it is consistent with the laws of quantum thermodynamics [41, 42]. It is only applicable for Markovian approximation. The solution $\rho(t)$ in Eq. (26) may be approximately found as a sequence of two steps: in the first step we make one step in the solution of the unitary part of Eq. (26)

$$\tilde{\rho}(t+dt) = \exp\left(-\frac{i}{\hbar}Hdt\right)\rho(t)\exp\left(\frac{i}{\hbar}Hdt\right) \quad (31)$$

and in the second step, make one step in the solution of Eq. (26) with the commutator removed

$$\rho(t+dt) = \tilde{\rho}(t+dt) + \frac{1}{\hbar}L(\tilde{\rho}(t+dt))dt \quad (32)$$

We obtain a updated $\rho(t+dt)$ in each iteration, substitute it into the equations of Sec. II, and obtain the corresponding entropy, concurrence and quantum discord.

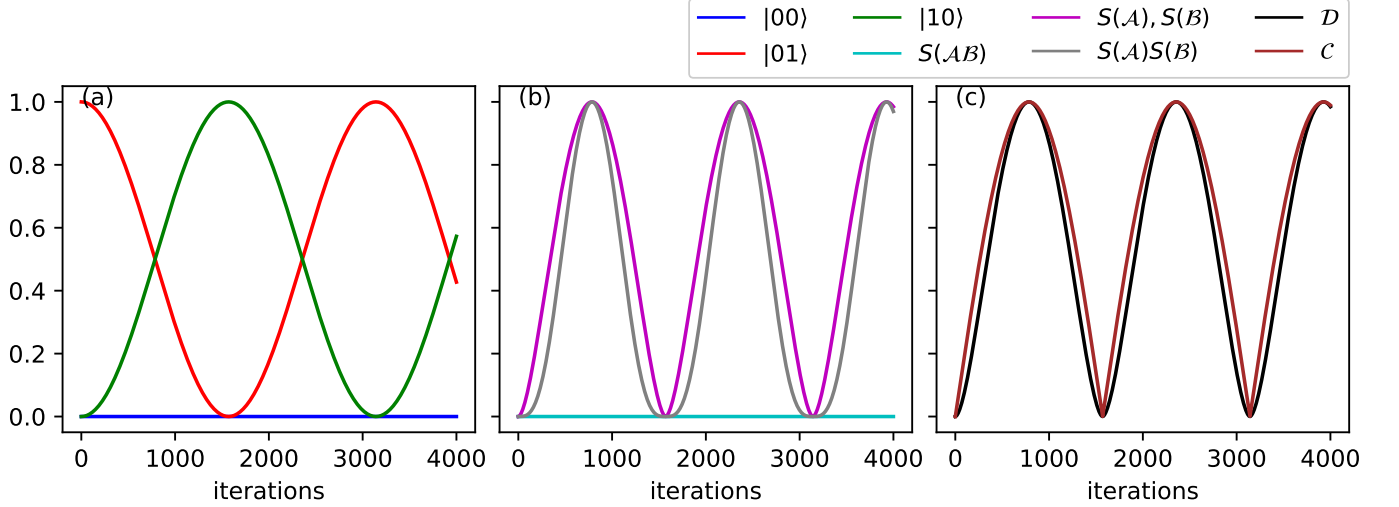


FIG. 4. (online color) *Quantum evolution and quantum correlation dynamics in closed system*. Here $\alpha = 0$, $\gamma = 0$. (a) shows the time-dependent curves of each state in the quantum evolution process. Entropies of whole system and its subsystems are shown in (b). Quantum discord and concurrence are shown in (c).

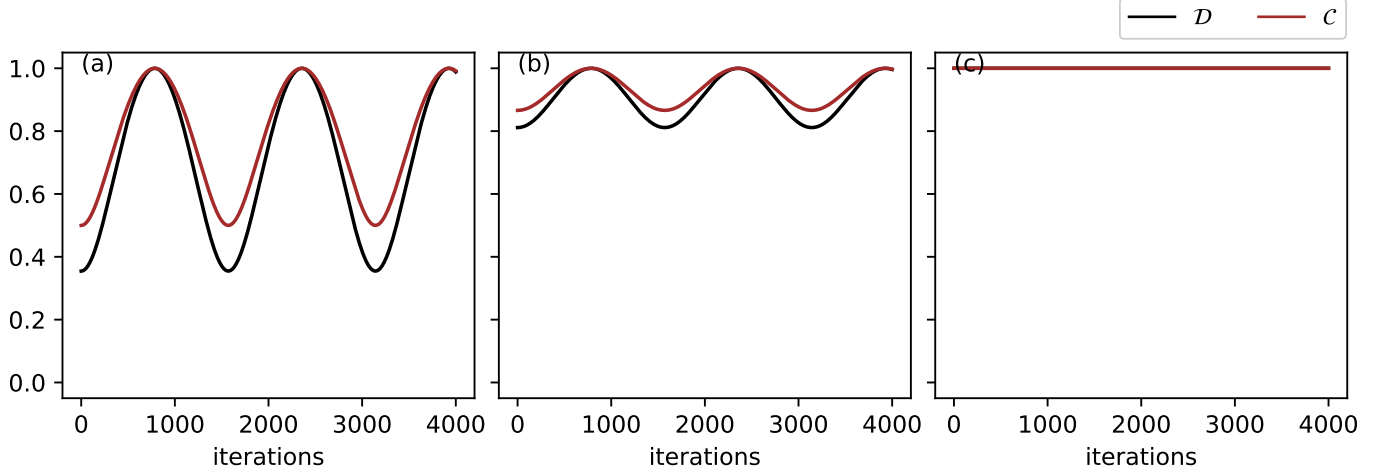


FIG. 5. (online color) *Quantum correlation dynamics in closed JCM with different initial entanglements*. $\gamma = 0$ in these cases. The case of $\alpha = 0$ is shown in Fig. 4 (c). Here (a) $\alpha = \frac{\pi}{12}$, (b) $\alpha = \frac{\pi}{6}$, (c) $\alpha = \frac{\pi}{4}$.

A. Two-qubit system

In simulations for two-qubit system: $\omega = 10^8$, $g = 10^6$. And the initial state is defined as follows

$$|\Psi(0)\rangle = \cos\alpha|01\rangle + \sin\alpha|10\rangle \quad (33)$$

where $\alpha \in [0, \frac{\pi}{4}]$.

1. Closed system

In Fig. 4, the initial state $|\Psi(0)\rangle = |01\rangle$ ($\alpha = 0$), and (a) \sim (c) are the results of the closed quantum system ($\gamma = 0$).

When the system is closed, the quantum evolution presents oscillation of $|01\rangle$ and $|10\rangle$ in Fig. 4 (a). At this time, the $|00\rangle$ is always 0, because there is no photon leakage, thus the $|00\rangle$ cannot be obtained through dissipation. We set the state of the entire system as

$$|\Psi\rangle = a|01\rangle + b|10\rangle \quad (34)$$

where $a^2 + b^2 = 1$.

In Fig. 4 (b), von Neumann entropy of entire system $S(\mathcal{AB})$ is always equal to 0, because whole system is pure state. At this time, for a bipartite system, $S(\mathcal{A})$ is always equal to $S(\mathcal{B})$. When coefficients a and b from Eq. (34) are equal, and $|\Psi\rangle = \frac{1}{\sqrt{2}}|01\rangle + \frac{1}{\sqrt{2}}|10\rangle$. The system

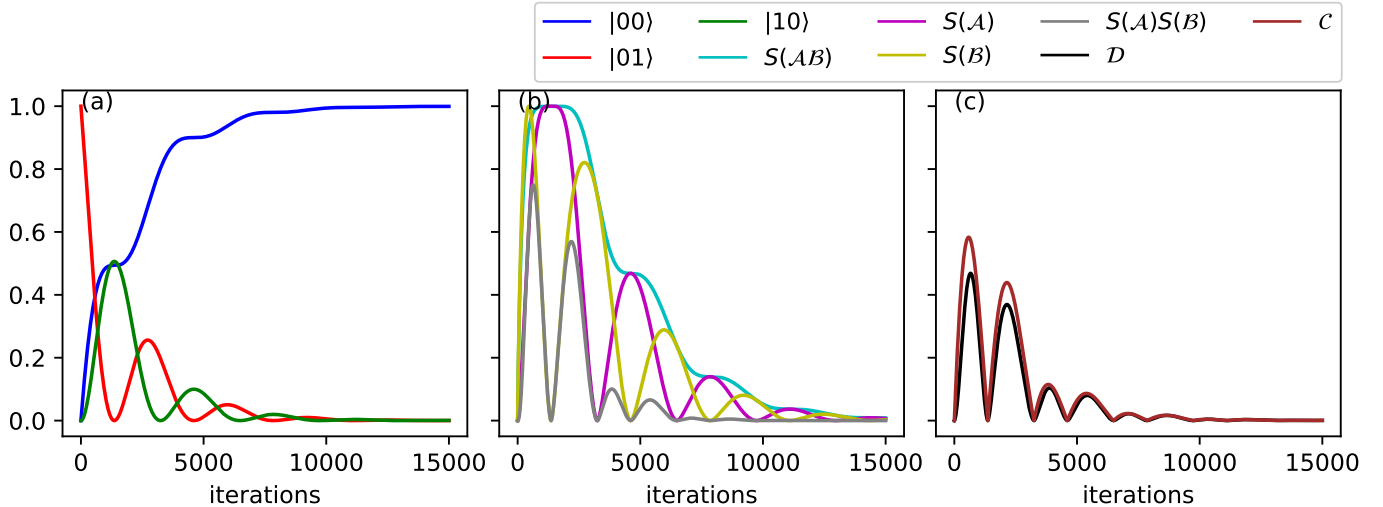


FIG. 6. (online color) *Quantum evolution and quantum correlation dynamics in open system*. Here $\alpha = 0$, $\gamma = g$.

reaches the maximum entanglement. We get that $S(\mathcal{A})$ ($S(\mathcal{B})$) is equal to 1 at this time, and the maximum value is obtained ($S_{max}(\mathcal{A}) = \log_2 N$, where $N = 2^n = 2$, because subsystem consists of a qubit ($n = 1$), thus $S_{max}(\mathcal{A}) = 1$). When $a = 1$, $b = 0$ (or $a = 0$, $b = 1$), the entanglement of system is 0. We get $S(\mathcal{A}) = S(\mathcal{B}) = 0$.

In Fig. 4 (c), concurrence, defined in Eq. (7), is introduced to measure quantum entanglement. Quantum discord, defined in Eq. (21), is introduced to measure quantum correlation. Like von Neumann entropy, both concurrence and quantum discord reach the maximum value 1 when the system is at the maximum entanglement degree, and reach 0 when quantum entanglement disappears. Moreover, concurrence and quantum discord are completely synchronized with von Neumann entropy.

Comparing the Fig. 4 (c) and Fig. 5 (a), (b) and (c), it can be found that when the initial entanglement degree is larger (α is larger), the lower limit of quantum discord and concurrence is larger. When α is 0, the initial entanglement degree is 0, and the lower limit is also 0 at this time, that is, the curves of quantum discord and concurrence oscillate between 0 and 1. As α becomes larger, the curves are gradually compressed towards the 1 boundary. Until α is $\frac{\pi}{4}$, the initial entanglement is the largest, and at this time the curves become horizontal lines that is always 1.

2. Open system

Now we focus on the open quantum system ($\gamma = g$). At this time, the whole system is no longer in the pure state. In Fig. 6 (a), due to the presence of photon leakage, the oscillation between the $|01\rangle$ and $|10\rangle$ not exists. Instead, the probability of $|00\rangle$ gradually increases from 0 to 1.

Now we set the state of the entire system as

$$|\Psi\rangle = a|01\rangle + b|10\rangle + c|00\rangle \quad (35)$$

where $a^2 + b^2 + c^2 = 1$. According to Fig. 6 (a), the probability of $|00\rangle$ is always non-zero when the evolution begins. And $a|01\rangle + c|00\rangle = (a+c)|0\rangle(a|1\rangle + c|0\rangle)$, which shows that it is not entangled. Similarly, $b|10\rangle + c|00\rangle = (b|1\rangle + c|0\rangle)(b+c)|0\rangle$, which are also not entangled. So the entanglement property of the whole system is still determined by $|01\rangle$ and $|10\rangle$.

In Fig. 6 (b), $S(\mathcal{A})$ and $S(\mathcal{B})$ are no longer coincident. This is because $S(\mathcal{A})$ is synchronized with $|10\rangle$ and $S(\mathcal{B})$ is synchronized with state $|01\rangle$. Therefore, when the system is closed, states $|10\rangle$ and $|01\rangle$ are synchronized, so $S(\mathcal{A})$ and $S(\mathcal{B})$ can coincide. But when the system is open, these two states are not synchronized, then $S(\mathcal{A})$ and $S(\mathcal{B})$ cannot coincide. Thus, von Neumann entropy cannot be used to accurately measure quantum entanglement. But we can try to multiply $S(\mathcal{A})$ and $S(\mathcal{B})$. At this time, $S(\mathcal{A})S(\mathcal{B})$ combines $S(\mathcal{A})$ (only synchronized with $|10\rangle$) and $S(\mathcal{B})$ (only synchronized with $|01\rangle$), which can be used to simply describe the entanglement of both closed (see gray curve in Fig. 4 (b)) and open quantum system (see gray curve in Fig. 6 (b)). In addition, $S(\mathcal{A})S(\mathcal{B})$ also synchronizes with quantum discord and concurrence in Fig. 6 (c).

According to quantum discord in Fig. 6, when there is photon leakage, the quantum correlation of the system will gradually weaken to 0 (at this point, the system only exists the state of $|00\rangle$).

Comparing the Fig. 4 (c), Fig. 6 (c) and Fig. 7 (a), (b), (c), it can be found that when the γ is larger, the oscillation of quantum discord and concurrence fade faster. Only when $\gamma = 0$, the oscillation always exists.

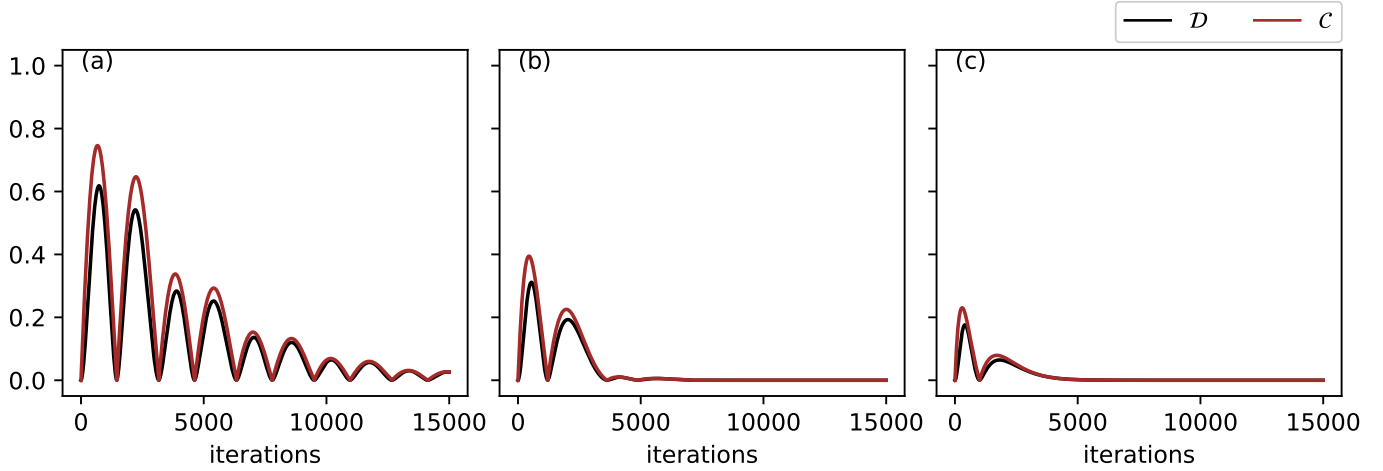


FIG. 7. (online color) *Quantum correlation dynamics in open JCM with different dissipation strengths.* $\alpha = 0$ in these cases. The cases of $\gamma = 0$ and $\gamma = g$ are shown in Fig. 4 (c) and Fig. 6 (c), respectively. Here (a) $\gamma = 0.5g$, (b) $\gamma = 2g$, (c) $\gamma = 4g$.

B. Three-qubit system

In simulations for three-qubit system: $\omega_c = \omega_a = 10^9$, $\omega_b = 10^8$, $g_{b_0} = 10^4$, $g_{b_1} = 100g_{b_0}$, $g_{a_1} = 2g_{b_1}$, $g_{a_0} = 100g_{a_1}$. And the initial state is defined as follows

$$|\Psi(0)\rangle = |100\rangle \quad (36)$$

In the initial condition, an electron is at ground-level, a photon is present in the cavity, and two atoms are far away from one another.

1. Quantum motion

In this simulation, g_{a_0} and g_{a_1} are both constants. g_{b_0} , and g_{b_1} are also constants due to the quantum motion of nuclei. The quantum movement of nuclei refers to the tunneling effect, that is, two atomic nuclei move from the close place to the far away place instantaneously. At this time, the intensities of covalent bond formation or breaking are constants. Likewise, movement of nuclei from the far away place to the close place is also instantaneous.

In Fig. 8, the inner figure shows quantum evolution of the OH^+ model with the dissipation of photon, associated only with electron transition. The evolution presents Rabi oscillation of states $|000\rangle$ and $|001\rangle$, other states quickly decay to 0. And the outer figure shows the quantum discord dynamics of this system. We can set the final state of entire system as

$$|\Psi\rangle = a|000\rangle + b|001\rangle \quad (37)$$

where $a^2 + b^2 = 1$. And $a|000\rangle + b|001\rangle = (a + b)|0\rangle(a|00\rangle + b|01\rangle)$, which shows that it's not entangled between subsystems \mathcal{A} and \mathcal{B} , defined in Eq. (29). Therefore, the quantum discord rises to 1 from the beginning, and then decays to 0 (at this time, only the

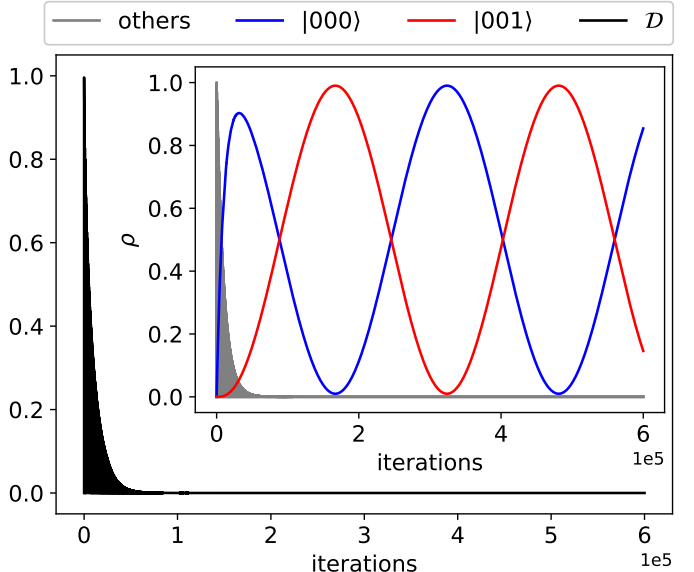


FIG. 8. (online color) *Quantum evolution and quantum discord dynamics in OH^+ model.* g_{b_0} , g_{b_1} , g_{a_0} and g_{a_1} are all constants. $|000\rangle$ is represented by blue curve and $|001\rangle$ is represented by red curve. Other states are all represented by the gray curves.

oscillations of $|000\rangle$ and $|001\rangle$ remain in the system) in violent oscillations.

2. Classical motion

In this simulation, g_{a_0} and g_{a_1} are also both constants, but g_{b_0} and g_{b_1} decrease gradually from maximum value to 0, at the same time, the movement of atomic nu-

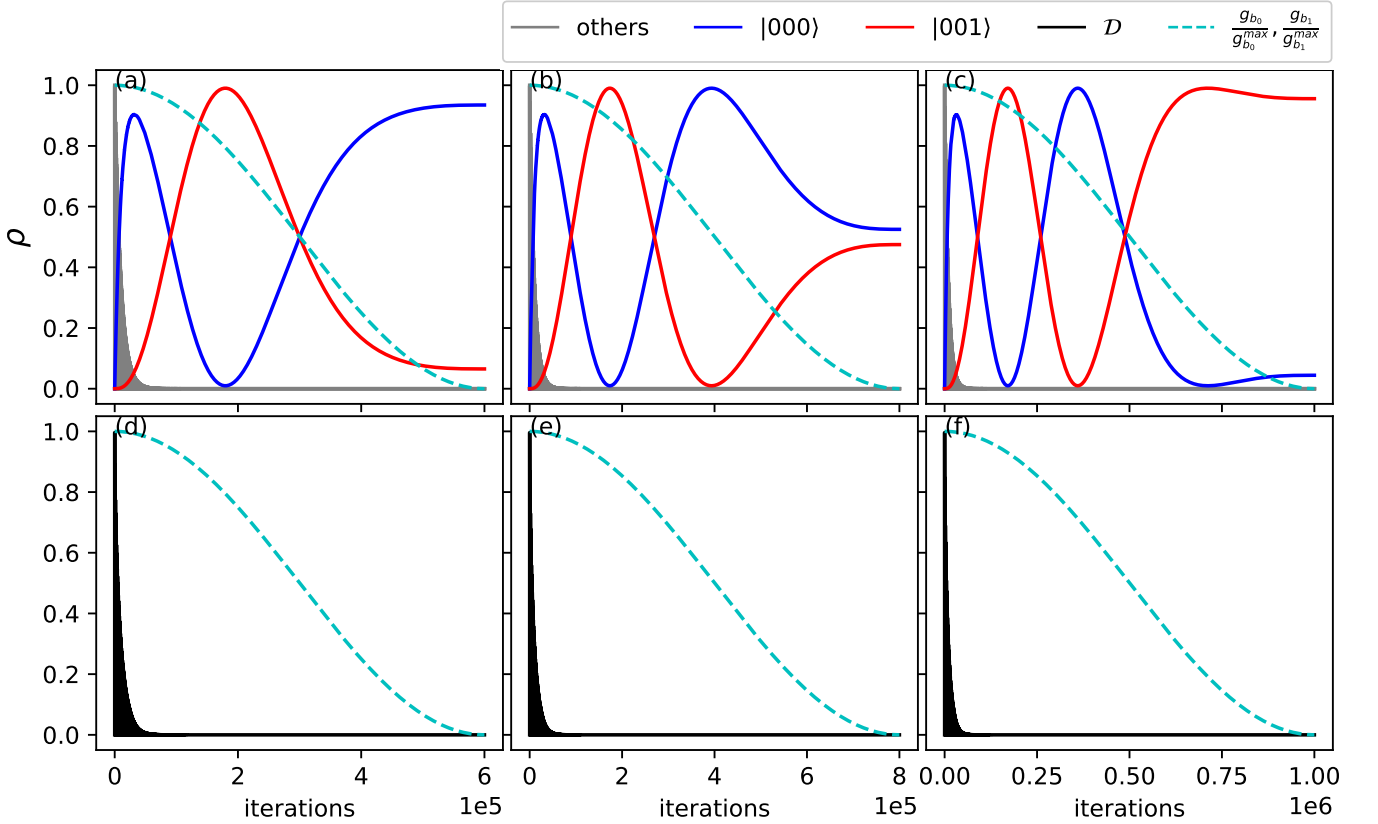


FIG. 9. (online color) *Quantum evolution and quantum discord dynamics in OH⁺ model.* g_{a_0} and g_{a_1} are constants, g_{b_0} and g_{b_1} decrease gradually from maximum values $g_{b_0}^{max}$ ($g_{b_1}^{max}$) to 0. Cyan dashed curve represents the ratio between g_{b_0} (g_{b_1}) and $g_{b_0}^{max}$ ($g_{b_1}^{max}$). The cases of different iteration numbers are (a) $6 * 10^5$, (b) $8 * 10^5$, (c) 10^6 . (d), (e) and (f) are the quantum discord dynamics corresponding to cases (a), (b) and (c), respectively.

clei gradually slowed down until it stopped. The biggest difference between the classical and quantum motion of atomic nuclei is that the classical motion refers to the slow movement of the nucleus from near to far, while the quantum motion refers to the repeated jumping of nuclei between the far away place and the close place due to the quantum tunneling effect.

From Fig. 9, we can see that as the number of iterations increases, g_{b_0} and g_{b_1} are getting smaller and smaller, the two nuclei are farther and farther apart, and the oscillation between $|000\rangle$ and $|001\rangle$ begins to deform (from vigorous to slow, in other words, the oscillation period becomes larger and larger). If the moving distance of the nuclei from near to far is constant, then the larger the superior limit of the number of iterations, the slower the nucleus moves. Comparing (a), (b) and (c), it can be found that the slower the movement, the more times the Rabi oscillations.

Now we focus on the quantum discord dynamics in Fig. 9 (d), (e) and (f). Whether it is quantum motion or classical motion, quantum dynamics is almost the same. This is because the classical motion only makes $|000\rangle$ and $|001\rangle$ deform significantly, and the oscillation of $|000\rangle$ and

$|001\rangle$ cannot cause the entanglement between subsystems \mathcal{A} and \mathcal{B} . At the same time, the deformation of other states is not obvious by classical motion.

VI. CONCLUDING DISCUSSION AND FUTURE WORK

In this paper, we simulate the quantum entanglement and quantum discord dynamics in the cavity QED models. We have derived some analytical results of it:

- In Sec. V A 1, we study two-qubit closed system of JCM. We found that quantum discord is synchronized with quantum entanglement (von Neumann entropy and concurrence). At the same time, it is found that the greater the initial entanglement degree, the higher the lower limit of the quantum discord and concurrence, preferably as the initial entanglement reaches the maximum, the quantum discord and concurrence becomes a horizontal line.
- In Sec. V A 2, we study two-qubit open system of JCM. We found that von Neumann entropies can-

not be used to describe the entanglement of the system, but concurrence can. In addition, we define $S(\mathcal{A})S(\mathcal{B})$, which may will be a good measure of the degree of entanglement in two-qubit open system. And quantum discord is synchronized with quantum entanglement (concurrence). At the same time, it is found that the greater the dissipation strength, the faster the quantum discord and concurrence decay.

- In Sec. V B 1, we have studied the quantum motion of atomic nuclei, and obtained that the quantum discord between subsystems \mathcal{A} and \mathcal{B} does not exist when the final system is in the oscillation of $|000\rangle$ and $|001\rangle$.
- In Sec. V B 2, we have studied the classical motion of atomic nuclei. According to findings, although classical motion gives a significant deformation to

the oscillations, the impact on quantum discord dynamics is negligible.

Although we only studied the quantum entanglement and quantum discord dynamics in the simplest cavity QED models via bipartite measurement, the results we found will be used as a basis to extend the research to more complex modifications of cavity QED model in the future.

ACKNOWLEDGMENTS

The reported study was funded by China Scholarship Council, project numbers 202108090327, 202108090483.

Appendix A: Abbreviations and notations

See Tab. I.

TABLE I: List of abbreviations and notations used in this paper.

Abbreviations/Notations Descriptions

EPR	Einstein–Podolsky–Rosen
QIP	Quantum information processing
QED	Quantum electrodynamics
JCM	Jaynes–Cummings model
TCM	Tavis–Cummings model
QME	Quantum master equation
RWA	Rotating wave approximation
$ \Psi\rangle$	Quantum state
$ \Psi(0)\rangle$	Initial state
\uparrow	Spin up
\downarrow	Spin down
\mathcal{AB}	Entire system, and $\mathcal{AB} \equiv \rho_{AB}$
\mathcal{A}	Observed subsystem, and $\mathcal{A} \equiv \rho_A$
\mathcal{B}	Substance subsystem, and $\mathcal{B} \equiv \rho_B$
E	Entanglement
S	Von Neumann entropy
ρ	Density matrix (e.g. ρ_{AB} , ρ_A , ρ_B , etc)
I_A	Unit operator
I_B	Unit operator
C	Concurrence
H	Information entropy
P	Probability
I	Mutual information
X	Variable

Continued on next page

– continued from previous page

Abbreviations/Notations	Descriptions
Y	Variable
\mathcal{I}	Quantum mutual information
\mathcal{J}	Maximum classical correlation
k	Outcome
k'	Outcome
Π_k^A	Projection operator on subsystem \mathcal{A}
$\Pi_{k'}^B$	Projection operator on subsystem \mathcal{B}
ρ_k	State of the subsystem \mathcal{B} after a measurement of subsystem \mathcal{A} leading to an outcome k
$\rho_{k'}$	State of the subsystem \mathcal{A} after a measurement of subsystem \mathcal{B} leading to an outcome k'
p_k	Probability of outcome k
$p_{k'}$	Probability of outcome k'
$\{ b_k\rangle\}$	Von Neumann measurement projective basis
θ	Radian corresponds to the qubit in observed subsystem
φ	Radian corresponds to the qubit in observed subsystem
\mathcal{D}	Quantum discord
ph	Photon
at	Atom
n	Nucleus
mol	Molecule
g	Coupling strength of photon and the electron
\hbar	Reduced Planck constant or Dirac constant
ω	Photonic mode, and $\omega = \omega_c = \omega_a$
ω_c	Cavity frequency
ω_a	Transition frequency
ω_b	Phononic mode
H_{JCM}^{RWA}	Hamiltonian of JCM
a	Photon annihilation operator, and its hermitian conjugate operator — a^\dagger
σ	Interaction operator of atom with the electromagnetic field of the cavity, and its hermitian conjugate operator — σ^\dagger
V	Effective volume of the cavity
d	Dipole moment of the transition between the ground and the perturbed states
$E(x)$	Spatial arrangement of the atom in the cavity
l	Length of the cavity
λ	Photon wavelength
γ_k	Total spontaneous emission rate for photon
A_k	Lindblad or jump operator of system, and its hermitian conjugate operator — A_k^\dagger
Φ_0	Bonding orbital or molecular ground orbital
Φ_1	Antibonding orbital or molecular excited orbital
O	Oxygen
H	Hydrogen

Continued on next page

– continued from previous page

Abbreviations/Notations	Descriptions
OH^+	Positive hydroxide
$H_{\text{OH}^+}^{RWA}$	Hamiltonian of OH^+ model

[1] A. Einstein, B. Podolsky, and N. Rosen, Can quantum-mechanical description of physical reality be considered complete?, *Phys. Rev.* **47**, 777 (1935).

[2] R. Horodecki, P. Horodecki, M. Horodecki, and K. Horodecki, Quantum entanglement, *Rev. Mod. Phys.* **81**, 865 (2009).

[3] M. Nielsen and I. Chuang, in *Quantum Computation and Quantum Information: 10th Anniversary Edition* (Cambridge University Press, Cambridge, 2010).

[4] A. K. Ekert, Quantum cryptography based on Bell's theorem, *Phys. Rev. Lett.* **67**, 661 (1991).

[5] C. H. Bennett, G. Brassard, C. Crépeau, R. Jozsa, A. Peres, and W. K. Wootters, Teleporting an unknown quantum state via dual classical and Einstein–Podolsky–Rosen channels, *Phys. Rev. Lett.* **70**, 1895 (1993).

[6] C. H. Bennett and S. J. Wiesner, Communication via one- and two-particle operators on Einstein–Podolsky–Rosen states, *Phys. Rev. Lett.* **69**, 2881 (1992).

[7] L. Henderson and V. Vedral, Classical, quantum and total correlations, *Journal of Physics A: Mathematical and General* **34**, 6899 (2001).

[8] H. Ollivier and W. H. Zurek, Quantum discord: A measure of the quantumness of correlations, *Phys. Rev. Lett.* **88**, 017901 (2001).

[9] W. H. Zurek, Quantum discord and Maxwell's demons, *Phys. Rev. A* **67**, 012320 (2003).

[10] V. Vedral, Classical correlations and entanglement in quantum measurements, *Phys. Rev. Lett.* **90**, 050401 (2003).

[11] B. Dakić, V. Vedral, and I. C. V. Brukner, Necessary and sufficient condition for nonzero quantum discord, *Phys. Rev. Lett.* **105**, 190502 (2010).

[12] J. Wang, J. Deng, and J. Jing, Classical correlation and quantum discord sharing of Dirac fields in noninertial frames, *Phys. Rev. A* **81**, 052120 (2010).

[13] F. F. Fanchini, L. K. Castelano, and A. O. Caldeira, Entanglement versus quantum discord in two coupled double quantum dots, *New Journal of Physics* **12**, 073009 (2010).

[14] Y.-H. Hu and M.-F. Fang, Quantum discord between two moving two-level atoms, *Open Physics* **10**, 145 (2012).

[15] M.-Q. Xie and B. Guo, Thermal quantum discord in heisenberg XXZ model under different magnetic field conditions, *Acta Phys. Sin.* **62**, 110303 (2013).

[16] K.-M. Fan and G.-F. Zhang, The dynamics of quantum correlation between two atoms in a damping Jaynes–Cummings model, *Acta Phys. Sin.* **62**, 130301 (2013).

[17] R.-Q. Li and D.-M. Lu, Quantum discord in the system of atoms interacting with coupled cavities, *Acta Phys. Sin.* **63**, 030301 (2014).

[18] S. M. Aldoshin, E. B. Fel'dman, and M. A. Yurishchev, Quantum entanglement and quantum discord in mag-

netoactive materials (review article), *Low Temperature Physics* **40**, 3 (2014).

[19] Z.-A. Jia, R. Zhai, S. Yu, Y.-C. Wu, and G.-C. Guo, Hierarchy of genuine multipartite quantum correlations, *Quantum Inf Process* **19**, 419 (2020).

[20] C. Radhakrishnan, M. Laurière, and T. Byrnes, Multipartite generalization of quantum discord, *Phys. Rev. Lett.* **124**, 110401 (2020).

[21] P. Brown, H. Fawzi, and O. Fawzi, Computing conditional entropies for quantum correlations, *Nat Commun* **12**, 575 (2021).

[22] E. Jaynes and F. Cummings, Comparison of quantum and semiclassical radiation theories with application to the beam maser, *Proceedings of the IEEE* **51**, 89 (1963).

[23] M. Tavis and F. W. Cummings, Exact solution for an N -molecule–radiation-field Hamiltonian, *Phys. Rev.* **170**, 379 (1968).

[24] D. G. Angelakis, M. F. Santos, and S. Bose, Photon-blockade-induced mott transitions and XY spin models in coupled cavity arrays, *Phys. Rev. A* **76**, 031805 (2007).

[25] H. Wei, J. Zhang, S. Greschner, T. C. Scott, and W. Zhang, Quantum monte carlo study of superradiant supersolid of light in the extended Jaynes–Cummings–Hubbard model, *Phys. Rev. B* **103**, 184501 (2021).

[26] S. Prasad and A. Martin, Effective three-body interactions in Jaynes–Cummings–Hubbard systems, *Sci Rep* **8**, 16253 (2018).

[27] L. Guo, S. Greschner, S. Zhu, and W. Zhang, Supersolid and pair correlations of the extended Jaynes–Cummings–Hubbard model on triangular lattices, *Phys. Rev. A* **100**, 033614 (2019).

[28] K. C. Smith, A. Bhattacharya, and D. J. Masiello, Exact k -body representation of the Jaynes–Cummings interaction in the dressed basis: Insight into many-body phenomena with light, *Phys. Rev. A* **104**, 013707 (2021).

[29] Y. I. Ozhigov, Space of dark states in Tavis–Cummings model, *Modern Information Technologies and IT Education* **15**, 27 (2019).

[30] R. Düll, A. Kulagin, W. Lee, Y. Ozhigov, H. Miao, and K. Zheng, Quality of control in the Tavis–Cummings–Hubbard model, *Computational Mathematics and Modeling* **32**, 75 (2021).

[31] A. Vitaliy, K. Zheng, K. Alexei, H. Miao, O. Yuri, L. Wanshun, and V. Nadezda, About chemical modifications of finite dimensional QED models, *Nonlinear Phenomena in Complex Systems* **24**, 230 (2021).

[32] H. hui Miao and Y. I. Ozhigov, Using a modified version of the Tavis–Cummings–Hubbard model to simulate the formation of neutral hydrogen molecule, *Physica A: Statistical Mechanics and its Applications* **622**, 128851 (2023).

- [33] H.-h. Miao and Y. I. Ozhigov, Comparing the effects of nuclear and electron spins on the formation of neutral hydrogen molecule, *Lobachevskii Journal of Mathematics* **44**, 3111 (2023).
- [34] C. H. Bennett, H. J. Bernstein, S. Popescu, and B. Schumacher, Concentrating partial entanglement by local operations, *Phys. Rev. A* **53**, 2046 (1996).
- [35] S. A. Hill and W. K. Wootters, Entanglement of a pair of quantum bits, *Phys. Rev. Lett.* **78**, 5022 (1997).
- [36] W. K. Wootters, Entanglement of formation of an arbitrary state of two qubits, *Phys. Rev. Lett.* **80**, 2245 (1998).
- [37] K. Audenaert, F. Verstraete, and B. De Moor, Variational characterizations of separability and entanglement of formation, *Phys. Rev. A* **64**, 052304 (2001).
- [38] Y. Wu and X. Yang, Strong-coupling theory of periodically driven two-level systems, *Phys. Rev. Lett.* **98**, 013601 (2007).
- [39] G. Rempe, H. Walther, and N. Klein, Observation of quantum collapse and revival in a one-atom maser, *Phys. Rev. Lett.* **58**, 353 (1987).
- [40] H.-P. Breuer, F. Petruccione, *et al.*, *The theory of open quantum systems* (Oxford University Press, 2002).
- [41] R. Alicki, The quantum open system as a model of the heat engine, *Journal of Physics A: Mathematical and General* **12**, L103 (1979).
- [42] R. Kosloff, Quantum thermodynamics: A dynamical viewpoint, *Entropy* **15**, 2100 (2013).